RSC Advances

Spin Mixed Charge Transfer States of Iridium Complex Ir(ppy)3: Transient Absorption and Time-Resolved Photoluminescence

Journal:	*RSC Advances*
Manuscript ID:	RA-ART-01-2015-001404.R1
Article Type:	Communication
Date Submitted by the Author:	20-Mar-2015

Complete List of Authors:	Mehata, Mohan; Delhi Technological University, Department of Applied Physics; Dalian Institute of Chemical Physics (DICP), Chinese Academy of Sciences, State Key Laboratory of Molecular Reaction Dynamics Yang, Yang; Dalian Institute of Chemical Physics (DICP), Chinese Academy of Sciences, State Key Laboratory of Molecular Reaction Dynamics Qu, Zongjin; Dalian Institute of Chemical Physics (DICP), Chinese Academy of Sciences, State Key Laboratory of Molecular Reaction Dynamics Chen, Junsheng; Dalian Institute of Chemical Physics (DICP), Chinese Academy of Sciences, State Key Laboratory of Molecular Reaction Dynamics Zhao, Feng-jiao; Dalian Institute of Chemical Physics (DICP), Chinese Academy of Sciences, State Key Laboratory of Molecular Reaction Dynamics Han, Ke-Li; Dalian Institute of Chemical Physics (DICP), Chinese Academy of Sciences, State Key Laboratory of Molecular Reaction Dynamics

Spin Mixed Charge Transfer States of Iridium Complex $Ir(ppy)_3$: Transient Absorption and Time-Resolved Photoluminescence

Mohan Singh Mehata[†,‡*], Yang Yang[†], Zongjing Qu[†], Jun-sheng Chen[†], Feng-jiao Zhao[†] and Ke-Li Han[†*]

[†]State Key Laboratory of Molecular Reaction Dynamics, Dalian Institute of Chemical Physics (DICP), Chinese Academy of Sciences, Dalian 116023, CHINA.

[‡]Laser-Spectroscopy Laboratory, Department of Applied Physics, Delhi Technological University, Bawana Road, Delhi 110042, INDIA.

[*]To whom correspondence should be sent: E-mail: (M.S. Mehata) msmehata@gmail.com; (Ke-Li Han) klhan@dicp.ac.cn.

ABSTRACT

Nanosecond transient absorption and time-resolved spectroscopic techniques were applied to study organometallic phosphorescent emitter $Ir(ppy)_3$ complex, tris[2-phenylpyridinato-C^2,N] iridium (III) dissolved in tetrahydrofuran (THF) under degassed conditions at ambient temperatures. Transient absorption curves obtained at the pump pulse of 355 nm and at probe wavelength of 430 - 600 nm show positive and negative signals, indicating triplet - triplet (T-T) absorption and triplet-singlet (T-S) emission. Tri-exponential global fitted transient absorption curves and time-resolved photoluminescence (PL) decays demonstrated the presence of four closed low lying triplet states, of which, two are emitting green PL with a lifetime of 210 ns and 1.71 µs. The emitting states are spin mixed metal-to-ligand charge transfer (^{3}MLCT) states produced from non-equilibrium ^{1}MLCT state following fast intersystem crossing (ISC), whereas the ^{1}MLCT state is produced directly and indirectly depending on excitation wavelength. Moreover, the electronic structures for the ground state and low-lying excited states of $Ir(ppy)_3$ were studied using quantum chemistry calculations.

Keywords: Transient absorption, time-resolved photoluminescence, DFT/TDDFT, Metal-to-ligand charge transfer (MLCT) states, Organometallic phosphorescent emitter $Ir(ppy)_3$.

INTRODUCTION

The green phosphorescent emitter $Ir(ppy)_3$ is known for the highly efficient photoluminescence (PL) and electroluminescence (EL) in organic light emitting devices (OLEDs). This is because phosphorescent materials, such as iridium complexes, can provide very high exciton formation efficiency of nearly 100% [1-4]. Such high quantum efficiencies result from efficient intersystem crossing because of strong spin-orbit coupling (SOC) of the iridium atom, which mixes the singlet (S) and triplet (T) states of the $Ir(ppy)_3$ complex, resulting in the large cross-section for visible absorption of the ground state and great molecular stability [4]. The fast intersystem crossings (~100 fs) from excited singlet to the triplet states result in nearly no fluorescence but a strong phosphorescence emission [5,6], a weak fluorescence is also reported at around ~400 nm [7]. The assignment of the emitting states is the low-lying metal-to-ligand charge transfer singlet (^{1}MLCT) and triplet (^{3}MLCT) states [2,5-15], in which an electron located in the metal based d-orbital transferred to the π orbital of ligand. The high quantum yield and molecular stability of Ir complexes make them suitable for diverse applications. Due to the importance of Ir complex $Ir(ppy)_3$ for green OLEDs, it is of great interests to study the electronic structure of the metal complex in more detail. Especially, the role of triplet substates in the strong PL and EL is worthy further investigation, which might hint some guidance for constructing more efficient OLEDs. Furthermore, application of external electric field to the $Ir(ppy)_3$ doped in a PMMA film under vacuum condition at different temperature (300 - 40 K) demonstrated two major effects- the Stark shifts and field-induced photoluminescence quenching [13]. The field-induced PL quenching which arises due to the decreased lifetime and the emitting state population is independent on excitation energy and temperature. The fundamental molecular parameters, e.g., changes in dipole moment and polarizability following

photoexcitation have also been reported [13]. Here, we used pump-probe technique and measured the nanosecond transient absorption spectra together with time-resolved PL spectra & PL decays in solvent under degassed conditions. The transient absorption together with time-resolved PL decay curves allow us to quantify the existence of low-lying singlet and triplet states, spin-mixed states, i.e., metal-to-ligand charge transfer (MLCT) states, which may or may not essentially emit photoluminescence. The low-lying excited states are intramolecular charge transfer states and possess ligand to ligand charge transfer (LLCT) and MLCT characters.

EXPERIMENTAL AND THEORETICAL METHODS

Tris(2-phenylpyridine)iridium (99%) tetrahydrofuran (99.9%) were procured from JK Chemical, China and used without further purification. Absorption spectra were recorded with Perkin-Elmer Lamda-35 spectrophotomer. Photoluminescence and time-resolved PL decay were recorded using Horiba Jobin Yuon FluoroMax-4 spectrofluorometer. Time-resolved PL decays were recorded using the time-correlated single photon counting method using LED as an excitation source. The decay data were analyzed using commercial software provided by Horiba.

Nanosecond transient absorption measurement was carried out using pump-probe techniques [15,16]. The pump pulse of 355 nm with pulse energy of 5mJ was generated by the third harmonic of a Nd-YAG laser. The pulse has full width half maximum (FWHM) of 10 ns and repetition rate 3 Hz (Initially 10 Hz, reduced by mechanical chopper). For probe light, xenon flash lamp was used and scanned over the wavelength range of 340 - 620 nm. The signal from the sample was led to the monochromater and then to PMT (Hamamatsu R928). The signal was averaged over 100 laser shots using a digital oscilloscope. All the samples

ware thoroughly degassed (N_2) prior to obtain absorption, PL, PL decay and transient absorption curves. Concentration of the samples was 2.5×10^{-5} M and the path length of the sample quartz cuvette is 10 mm.

Ground-state geometry optimizations were carried out using DFT methods with the Cam-B3LYP functional, which is widely used in large-molecule systems. All excited-state calculations were performed using TDDFT methods with the Cam-B3LYP functional. All quantum calculations were performed with the Gaussian 09 program [17], and solvent effects were included using the integral equation formalism (IEF) version of polarizable continuum model (PCM) with the dielectric constant of tetrahydrofuran (ε = 7.52). Throughout the ground-state optimizations and excited-state studies, the SVP basis set was chosen for nonmetallic elements and the LanL2dz basis set was selected for iridium atoms, which is widely used in metal complexes [16,18,19].

RESULTS AND DISCUSSION

Figure 1 shows steady-state absorption, PL and PL excitation spectra of $Ir(ppy)_3$ in THF. Absorption shows strong bands at around 375 nm and 285 nm. The PL spectrum shows a maximum band at 512 nm with a small hump at 540 nm. Both the absorption and PL/phosphorescence are nearly the same as those observed in PMMA polymer film [13] and in solvents [5,6]. At low temperature of 40 K, the hump is well resolved [13]. The maximum PL intensity is observed at longer excitation wavelength (375 nm), which decreases with shortened excitation wavelength. As an example, the PL intensity observed at 285 nm excitation is one third that of at 375 nm, indicating the indirect (285 nm) and direct (355/376 nm) excitation of the metal-to-ligand charge transfer states. Thus, the steady-state

absorption represents to the locally excited (LE) singlet (higher energy band) and MLCT states (lower energy band) transitions.

Figure 2 shows the transient absorption spectrum of $Ir(ppy)_3$ measured at 355 nm (5mJ/per pulse) excitation in THF under degassed conditions. The pulse energy was kept as low as possible to obtain the transient signal so that two photon excitation and photochemical decomposition can be avoided. A series of absorption and emission peaks lasts for several micro-seconds. The strongest absorption and emission peaks appear at 530 nm and 550 nm, respectively attributed to the triplet-triplet (T-T) absorption and triplet-single (T-S) emission of $Ir(ppy)_3$. It is important to note that both absorption and emission signals appear in the similar wavelength region and are nearly overlapped.

Figure 3 shows transient absorption dynamical curves of $Ir(ppy)_3$ observed at different probe wavelengths. The dynamical curves were obtained at every 10 nm interval in the 430-620 nm region yet only four dynamical curves at 370, 410, 520 and 540 nm are selected as the multiple data sets due to their high signal to noise ratio (Fig. 3). The dynamical curves have both positive and negative lobes at each probe wavelength, indicating that both absorption (T-T) and emission (T-S) occur at each selected probed wavelength. Then the transient absorption curves could be simulated by the linear combination of absorption and emission using global fit method [15]. The global fittings were performed to get the accurate lifetimes. All the transient absorption curves are well fitted with tri-exponential fit components: $\Delta Abs(t) = A_1\ exp(-t/\tau_1) + A_2\ exp(-t/\tau_2) + A_3\ exp(-t/\tau_3)$ wherein τ_1, τ_2, and τ_3 are the lifetimes and A_1, A_2 and A_3 are the pre-exponential factors. The fitted lifetime are 1.72 ± 0.01, 1.71 ± 0.01 and 1.71 ± 0.01 μs with the adjustment R^2 of 0.96. Note that the observed transient curves could not simulated with considering mono- and bi-exponential functions, i.e., both mono- and bi-exponential

functions could not give reasonable fitting (supplementary information Table S2 and Fig. S1). The pre-exponential factor varies with probe wavelength and one of the pre-exponential factors is negative at each probe wavelength (Supplementary information Table S1). The lifetime corresponds to positive amplitude indicating to the T-T transitions/absorption and the negative value indicates to the T-S transitions, the light emitting state. We could not observed PL from ^{1}MLCT states because of the fast and strong ISC from ^{1}MLCT to ^{3}MLCT. The tri-exponential fitted curves clearly indicating the existence of three triplet (^{3}MLCT) states of $Ir(ppy)_3$ complex, which has nearly equal lifetime, of which, one of the T-state (^{3}MLCT) emits green photoluminescence.

The excited state dynamics of $Ir(ppy)_3$ complex dissolved in THF were further examined. This was done by the measurement of PL decay profiles with 376 nm excitation and monitored at 510 nm emission wavelength under degassed condition, as shown in Fig. 4 (black line). The decay profiles were simulated by assuming a bi-exponential decay, i.e., $A_4\, exp(-t/\tau_4) + A_5\, exp(-t/\tau_5)$, and lifetimes and pre-exponential factors were determined. The fitted lifetime and pre-exponential factor are τ_4 = 203.65 $\pm$ 0.26 (99.71 $\pm$ 0.0004) ns and τ_5 = 13.08 $\pm$ 0.29 (0.29 $\pm$ 0.002) ns and the average lifetime $\tau_{av} = \Sigma_i A_i\tau_i / \Sigma_i A_i$ is 203 ns. The amplitude of τ_5 is very small (as given in parenthesis, ~0.3%) and the observed decay is nearly single exponential with a lifetime of τ = 210.57 $\pm$ 0.20 ns. Note that the lifetime observed in non-degassed THF is approximately one tenth that observed in degassed THF (*c.f.,* Fig. 4), indicating the lifetime of $Ir(ppy)_3$ is quenched largely by oxygen. Similar trend is observed for PL intensity. This indicates that the PL/EL efficiency of $Ir(ppy)_3$ may be tuned by the concentration of oxygen present in the solution/micro-environment or dissolve oxygen can be monitored by the measurement of PL intensity and PL decay curves in 10 - 300 ns time regime.

In general, an exponential decay time of 1-2 μs was observed in solution, depending on the solvents used [2,10,20,21]. In PMMA film, a bi-exponential decay with decay times of 0.563 ± 0.003 (0.283 ± 0.001) μs and 1.460 ± 0.002 (0.717 ± 0.002) μs were observed [13]. In neat film, a faster non-exponential decay whose average lifetime is shorter by one order of magnitude than that in solution was observed [21-25]. It has also been reported that the PL from $Ir(ppy)_3$ micro-rods and nanowires decays much faster than that in degassed solution and in PMMA film [26]. Thus, the lifetime of $Ir(ppy)_3$ is critically depending on the micro-environment around the metal complex. Both mono- and bi-exponential decays were observed in solvents and polymer films in time-resolved PL decay measurement. Based on temperature dependence decays and magnetic field dependence PL spectra it was considered that the triplet state has three substates, which emits PL [9,10]. Hofbeck and Yersin [9] have reported 0-0 transitions of the three triplet substates with the decay time of 116 μs, 6.4 μs and 200 ns at B=0 (zero magnetic field). Out of which, the substate III (200 ns) represents the most important substate for the radiative properties. The decay time of the state varies between 200 and 600 ns, even shorter [24,25].

As discussed, the emitting state of $Ir(ppy)_3$ is not purely a triplet state but the PL originates from low lying spin-mixed metal-to-ligand charge transfer (MLCT) states; initially a charge-separated state (^{1}MLCT) is produced following photo-excitation and finally an equilibrium ^{3}MLCT states were formed following fast ISC with a time constant of ~100 fs [5,6]. The enhancement in the excited state dipole moment also indicates the charge-transfer character following absorption transitions [13]. The transient absorption together with PL decay analysis clearly indicate the existence of four closely lying spin mixed ^{3}MLCT states of $Ir(ppy)_3$ complex, of which, two are emitting PL with a lifetime of 100 - 600 ns and 1-2 μs. We could not observe the smaller lifetime components in transient absorption, as

the time resolution of our setup is ~100 ns. Moreover, the possibility of the fourth triplet substate, which occurs in the thermally accessible energy range at 300 K is also supported [10].

DFT AND TDDFT CALCULATIONS

The optimized structures of ground, first excited singlet and first triple states are shown in Fig. 5. The calculated electronic transition energies and corresponding oscillator strength (*f*) of the low-lying singlet excited states are listed in Table 1, which show that the longest wavelength absorptions of $Ir(ppy)_3$ complex are at 353, 344, 326, 318, 307 and 300 nm, respectively. The calculated vertical excitation energy of the first singlet transition is 353 nm, which corresponds to the experiment absorption at 375 nm. This indicates that the calculation method is reliable [16].

As shown in Table 1, the bright state (S1) corresponds to the orbital transition of the highest occupied molecular orbital (HOMO) to the lowest unoccupied molecular orbital (LUMO) and the HOMO to the LUMO + 2 ($f \approx 0.13$). The (S2) state corresponds to the orbital transition of the HOMO to the LUMO + 1 or the HOMO to the LUMO + 2. Similarly, other transitions are shown in Table 1. The frontier molecular orbitals spanning from HOMO-1 to the LUMO + 2 are involved in these transitions. The calculated frontier molecular orbital and the corresponding orbital energies for the organometallic compound $Ir(ppy)_3$ are shown in Fig. 6. One can see that the first singlet transitions, i.e., low lying excited state is intramolecular charge transfer state and it possess metal-to-ligand charge transfer (MLCT) and ligand-to-ligand charge transfer (LLCT) characters. Except the (S2) state, all the higher transitions possess both the MLCT and LLCT characters (Table 1). The second excited state (S2) possesses only LLCT character. The charge transfer character of low-lying excited states

of $Ir(ppy)_3$ complex was also discussed, based on electric field modulation spectroscopy [13]. Direct relaxation from the low-lying bright state (S1) to the ground sate could not detect as photoluminescence but populated low-lying spin mixed triplet states following fast ISC, this is because of the heavy metal Ir ions which enhance the ISC effects. It has been mentioned [11,27,28] that strong SOCs are obtained among the low-lying excited singlet and triplet states, and fast intersystem crossing into the low-lying excited spin-mixed states, based on quantum chemistry calculations. The emission may occur from the third and fifth spin-mixed states, i.e., sublevels of T_1, into the lowest spin-mixed state (ground state). On the other hand, on the basis of the assumption that radiative processes obey Fermi' Golden rule, large transition probabilities are obtained between the sublevels of the adiabatic lowest triplet (T_1) state and the ground (S_0) state [11,27].

CONCLUSIONS

We investigated photophysical properties of organometallic complex $Ir(ppy)_3$ using transient absorption and time-resolved photoluminescence spectroscopic experiments together with quantum chemistry calculations. The transient absorption spectrum/dynamical curves show both positive and negative lobes, indicating to the T-T and T-S transitions, respectively. The fitted transient absorption dynamical and PL decay curves indicate the existence of four closed low-lying spin mixed metal-to-ligand charge transfer (^{3}MLCT) states, of which, two are emitting photoluminescence with lifetimes of 211 ns and 1.71 µs. PL from ^{1}MLCT state is absent due to the fast ISC between ^{1}MLCT and ^{3}MLCT states. Furthermore, we calculated the electronic structures for the ground and low-lying excited state of $Ir(ppy)_3$ complex using DFT/TDDFT methods. The optimized structure in ground, first excited singlet and triplet states were obtained. The low-lying excited-state transition computational results indicated

the (S1) is brightest state among all the higher excited states, and the low lying excited states have charge transfer characters. Thus, the knowledge about the existence of multiple emitting states, spin-mixed charge transfer states is important for improving its application in OLEDs.

ACKNOWLEDGEMENTS

MSM thanks Chinese Academy of Science (CAS), China for supporting his stay at DICP, CAS, Dalian, China under CAS visiting scholar program and DAE-BRNS (No. 2012/37P/20/BRNS/765) Govt. of India. This work is financially supported by the National Basic Research Program of China (2013CB834604) and Natural Science Foundation of China (NSFC) (Grants No.21403226).

REFERENCES

1. C. Adachi, M. A. Baldo, M. E. Thompson and S. R. Forrest, *J. Appl. Phys*., 2001, **90**, 5048.
2. K. A. King, P.J. Spellane and R. J. Watts, *J. Am. Chem. Soc*., 1985, **107**, 1431.
3. K. Dedeian, P. I. Djurovich, F. O. Garces, G. Carlson and R. J. Watts, *Inorg. Chem.,* 1991, **30**, 1685.
4. X. H. Yang and D. Neher, *Appl. Phys. Lett.,* 2004, **84,** 2476.
5. K-C. Tang, K.L. Liu and I-C. Chen, *Chem. Phys. Lett.,* 2004, **386**, 437.
6. G.J. Hedley, A. Ruseckas and I.D.W. Samuel, *Chem. Phys. Lett*., 2008, **450**, 292.
7. Y. Koide, S. Takahashi and M. Vacha, *J. Am. Chem. Soc.,* 2006, **128**, 10990.
8. M.G. Colombo, T.C. Brunold, T. Riedener and H.U. Gudel, *Inorg. Chem*., 1994, **33**, 545.
9. T. Hofbeck and H. Yersin, *Inorg. Chem.,* 2010, **49**, 9290.

10. W. J. Finkenzeller and H. Yersin, *Chem. Phys. Lett.*, **2003**, 377, 299.
11. P. J. Hay, *J. Phys. Chem. A* 2002, **106**, 1634.
12. C. Nemirow, J. Fine, Z. Lu, K. Diri, A.I. Krylov and C. Wittig, *Mol. Phys.,* **2012**, 110, 1893.
13. M. S. Mehata and N. Ohta, *Appl. Phys. Lett.* 2011, **98**, 181910.
14. G. J. Zhao, K. L. Han, *Acc. Chem. Res.*, 2012, **45**, 404.
15. Y. Yang, L. Liu, H. Yin, D. Xu, G. Liu, X. Song and J. Liu, *J. Phys. Chem. C*, 2013, **117**, 11858.
16. J.S. Chen, G. J. Zhao, T.R. Cook, K.L. Han and P.J. Stang, *J. Am. Chem. Soc.*, 2013, **135**, 6694.
17. M.J. Frisch, G.W. Trucks, H.B. Schlegel, G.E. Scuseria, M.A. Robb, J.R. Cheeseman, G. Scalmani, V. Barone, B. Mennucci, G.A. Petersson, H. Nakatsuji, M. Caricato, X. Li, H.P. Hratchian, A.F. Izmaylov, J. Bloino, G. Zheng, J.L. Sonnenberg, M. Hada, M. Ehara, K. Toyota, R. Fukuda, J. Hasegawa, M. Ishida, T. Nakajima, Y. Honda, O. Kitao, H. Nakai, T. Vreven, J.A. Jr. Montgomery, J.E. Peralta, F. Ogliaro, M. Bearpark, J.J. Heyd, E. Brothers, K.N. Kudin, V.N. Staroverov, T. Keith, R. Kobayashi, J. Normand, K. Raghavachari, A. Rendell, J.C. Burant, S.S. Iyengar, J. Tomasi, M. Cossi, N. Rega, J.M. Millam, M. Klene, J.E. Knox, J.B. Cross, V. Bakken, C. Adamo, J. Jaramillo, R. Gomperts, R.E. Stratmann, O. Yazyev, A.J. Austin, R. Cammi, C. Pomelli, J.W. Ochterski, R.L. Martin, K. Morokuma, V.G. Zakrzewski, G.A. Voth, P. Salvador, J.J. Dannenberg, S. Dapprich, A.D. Daniels, O. Farkas, J.B. Foresman, J.V. Ortiz, J. Cioslowski, D.J. Fox, Gaussian 09, Revision C.01, Gaussian Inc, Wallingford CT, 2010.
18. G. J. Zhao, B. H. Northrop, P. J. Stang and K. L. Han, *J. Phys. Chem. A*, 2010, **114**, 3418.
19. G. J. Zhao, B. H. Northrop, K. L. Han and P. J. Stang, *J. Phys. Chem. A,* 2010, **114**, 9007.

20. A. Endo, K. Suzuki, T. Yoshihara, S. Tobita, M. Yahiro and C. Adachi, *Chem. Phys. Lett.,* 2008, **460**, 155.

21. E. B. Namdas, A. Ruseckas, I. D. W. Samuel, S. C. Lo and P. L. Burn, *J. Phys. Chem. B,* 2004, **108**, 1570.

22. C. Adachi, M. A. Baldo, S. R. Forrest and M. E. Thompson, *Appl. Phys. Lett.*, 2000, **77**, 904.

23. J. Kalinowski, W. Stampor, M. Cocchi, D. Virgili, V. Fattori and P. Di Marco, *Chem. Phys.,* 2004, **297**, 39.

24. A. Endo and C. Adachi, *Chem. Phys. Lett.,* 2009, **483**, 224

25. J. H. Seo, N. S. Han, H. S. Shim, J. H. Kwon and J. K. Song, *Bull. Korean Chem. Soc. 2011*, 32, 1415.

26. H. Wang, Q. Liao, H. Fu, Yi Zeng, Z. Jiang, J. Ma and J. Yao, *J. Mater. Chem.,* 2009, **19**, 89.

27. T. Matsushita, T. Asada and S. Koseki, *J. Phys. Chem. C*, 2007, **111**, 6897.

28. J. M. Younker and K. D. Dobbs, *J. Phys. Chem. C,* **2013**, 117, 25714.

Table 1. Selected calculated electronic transition energies and corresponding oscillator strengths of the low-lying singlet excited states of $Ir(ppy)_3$ complex

Electronic transition	**Energy (nm/eV)**	**Oscillator strength**	**Contribution**	**CI %**	**Character**
$S_0 \rightarrow S_1$	353 (3.51)	0.1326	H →L	63.4	MLCT
			H→L+2	20.0	LLCT
$S_0 \rightarrow S_2$	344 (3.60)	0.0025	H →L+1	36.3	LLCT
			H→L+2	48.6	LLCT
$S_0 \rightarrow S_3$	326 (3.81)	0.0379	H-1 →L+1	19.5	MLCT
			H →L+1	30.9	LLCT
			H →L	16.6	MLCT
$S_0 \rightarrow S_4$	318 (3.90)	0.0842	H-1→L	25.9	MLCT
			H-1 →L+1	36.7	LLCT
			H→L+1	16.0	LLCT
$S_0 \rightarrow S_5$	307 (4.04)	0.0126	H-1→L	52.5	MLCT
			H-1→L+1	31.7	LLCT
$S_0 \rightarrow S_6$	300 (4.13)	0.0656	H-1→L+2	78.0	MLCT

H stands for highest occupied molecular orbital (HOMO) and L for lowest unoccupied molecular orbital (LUMO). MLCT stands for metal-to-ligand charge transfer and LLCT for ligand-to-ligand charge transfer.

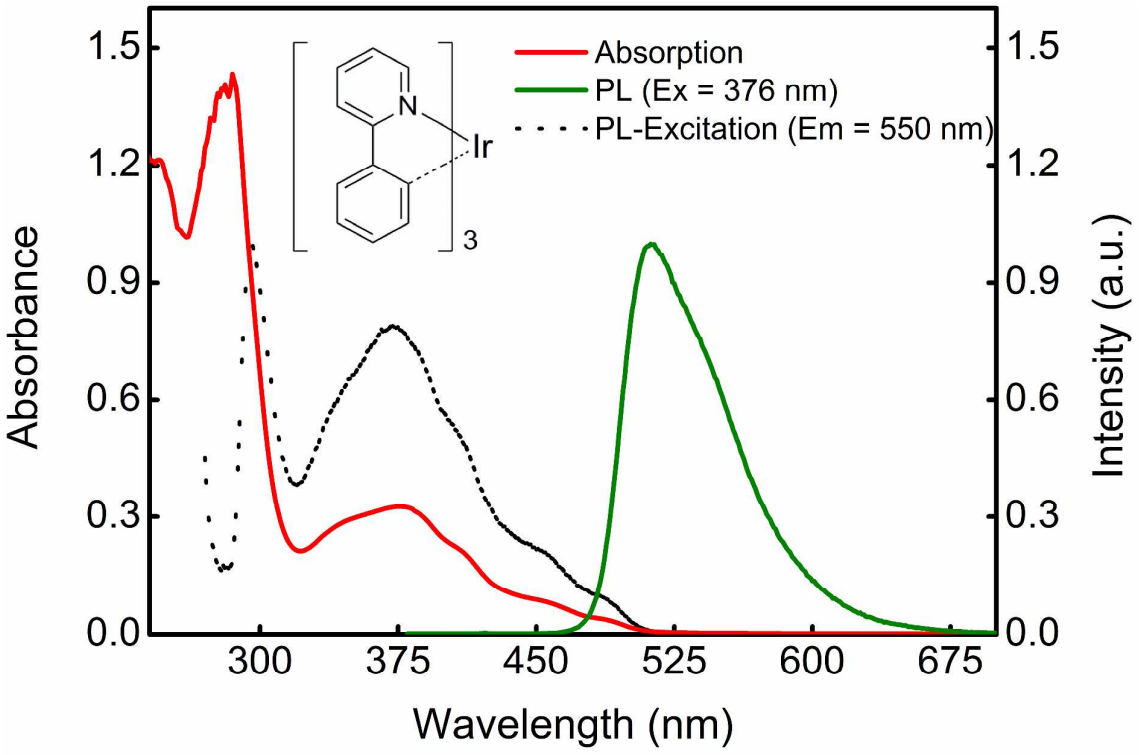

Figure 1: Normalized steady-state absorption, PL and PL-excitation spectra of a $Ir(ppy)_3$ dissolved in THF under degassed condition. Excitation and emission wavelength were 376 nm and 550 nm, respectively. Insert shows the structure of $Ir(ppy)_3$.

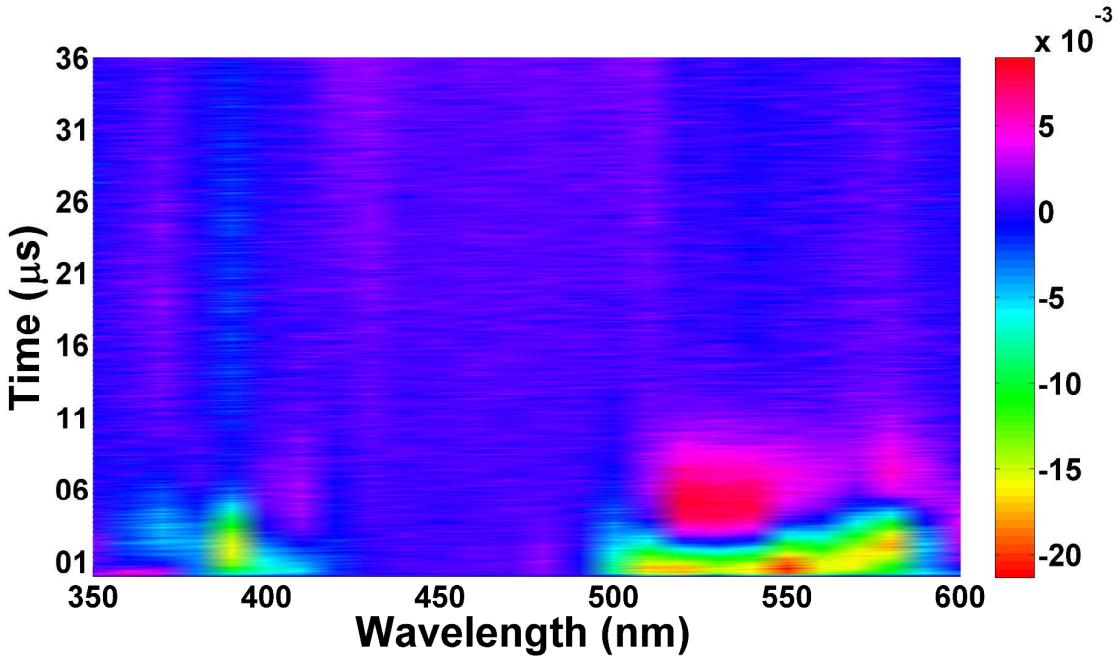

Figure 2: Transient absorption spectrum of $Ir(ppy)_3$ as a function of probe wavelength in THF under degassed conditions. Pumped wavelength was 355 nm with pulse energy of 5 mJ.

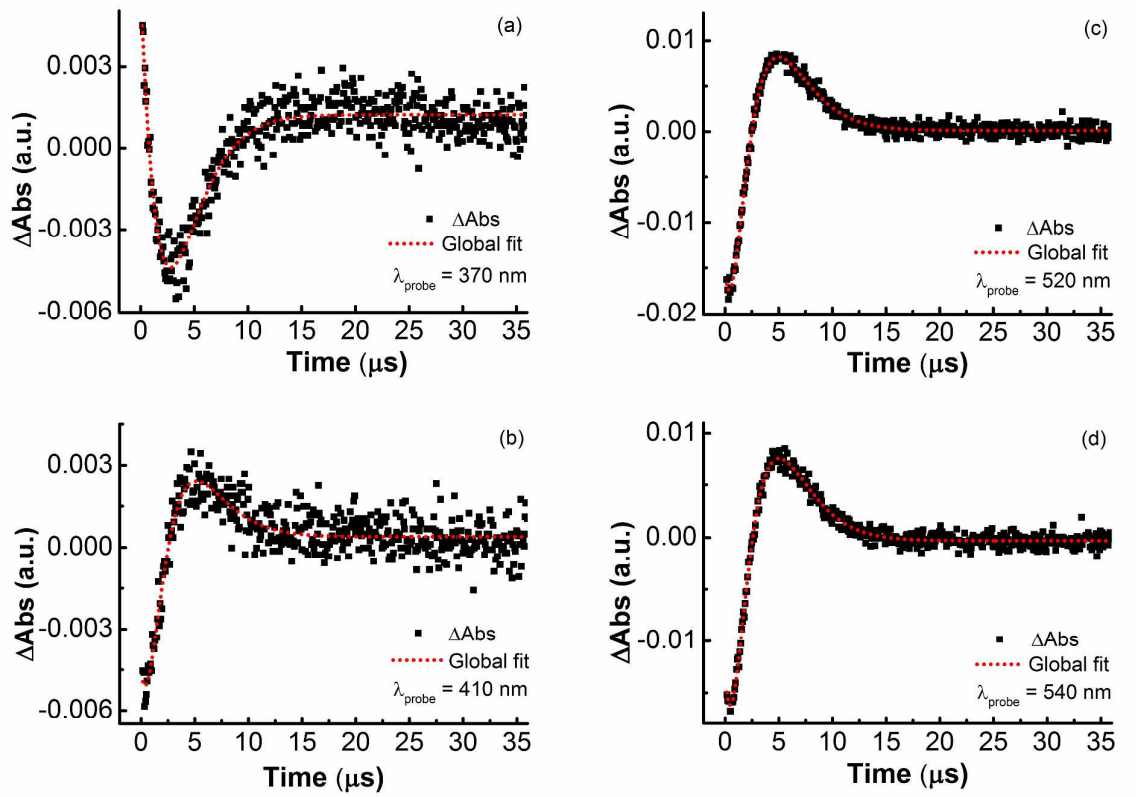

Figure 3: Transient absorption dynamical curves/absorbance (ΔAbs) of $Ir(ppy)_3$ in THF at probe wavelengths of (a) 370, (b) 410, (c) 520 and (d) 540 nm pumped by a nanosecond laser pulses of 355 nm@5mJ under degassed conditions. The black and red curves stand for the original data (solid black) and the global fit (dotted red), respectively.

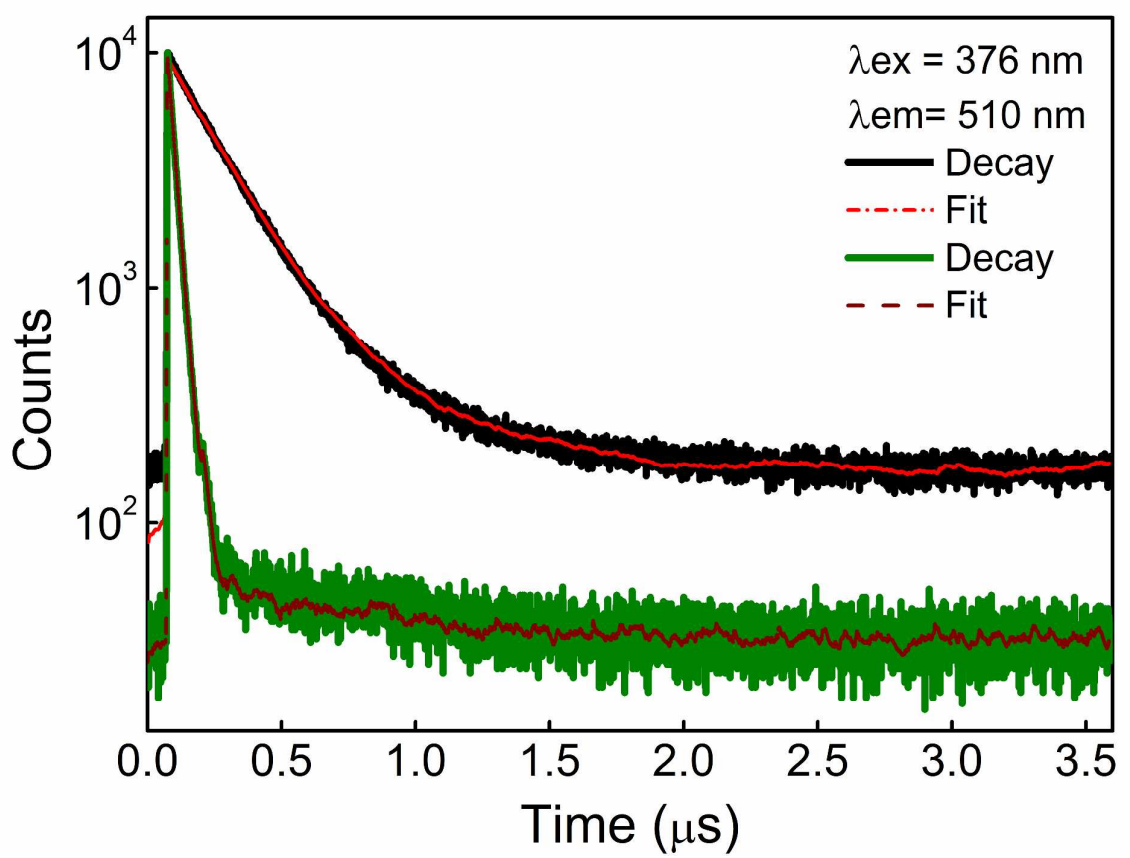

Figure 4: Photoluminescence decay curves of $Ir(ppy)_3$ in THF (solid black line) observed at 298 K under degassed condition and simulated curve (dotted red line). Excitation and emission wavelengths were 376 and 510 nm, respectively. The PL decay curve (solid green line) and simulated curve (dotted red line) observed under non-degassed condition.

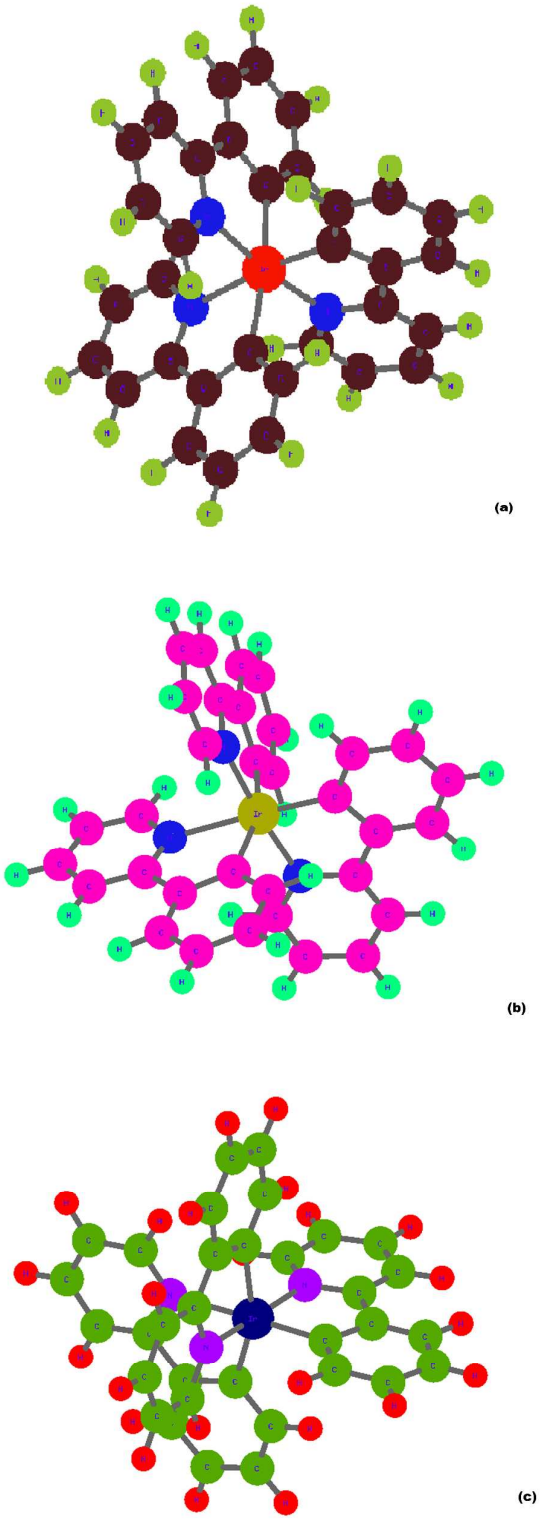

Figure 5: (a) The optimized ground state (S_0), (b) the first singlet excited state (S_1) and (c) the first triplet excited state (T_1) structures of $Ir(ppy)_3$.

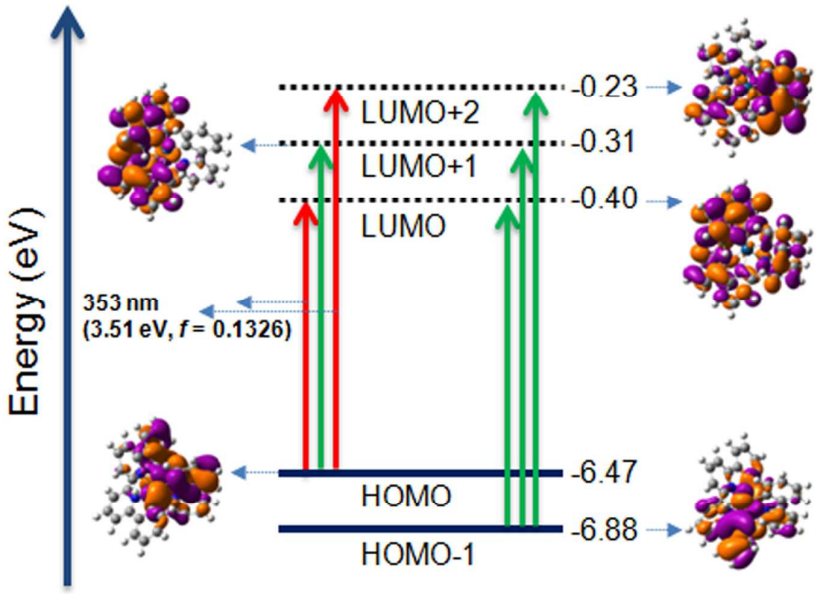

Figure 6: The calculated frontier molecular orbitals for the low-lying bright states of $Ir(ppy)_3$.